Appendix A

Antenna Theory and Design

SECOND EDITION

Warren L. Stutzman
Gary A. Thiele

JOHN WILEY & SONS, INC.
New York • Chichester • Weinheim • Brisbane • Toronto • Singapore

2.3.2 Monopoles

The principles of image theory are illustrated in this section with several forms of the monopole antenna. A **monopole** is a dipole that has been divided in half at its center feed point and fed against a ground plane. Three monopoles and their images in a perfect ground plane are shown in Fig. 2-11. High-frequency monopoles are often fed from coaxial cables behind the ground plane as shown in Fig. 2-12*a*.

The currents and charges on a monopole are the same as on the upper half of its dipole counterpart, but the terminal voltage is only half that of the dipole. The voltage is half because the gap width of the input terminals is half that of the dipole, and the same electric field over half the distance gives half the voltage. The input impedance for a monopole is therefore half that of its dipole counterpart, or

$$Z_{A,\text{mono}} = \frac{V_{A,\text{mono}}}{I_{A,\text{mono}}} = \frac{\frac{1}{2}V_{A,\text{dipole}}}{I_{A,\text{dipole}}} = \frac{1}{2}Z_{A,\text{dipole}} \tag{2-17}$$

This is easily demonstrated for the radiation resistance. Since the fields only extend over a hemisphere, the power radiated is only half that of a dipole with the same current. Therefore, the radiation resistance of a monopole is given by

$$R_{r,\text{mono}} = \frac{P_{\text{mono}}}{\frac{1}{2}|I_{A,\text{mono}}|^2} = \frac{\frac{1}{2}P_{\text{dipole}}}{\frac{1}{2}|I_{A,\text{dipole}}|^2} = \frac{1}{2}R_{r,\text{dipole}} \tag{2-18}$$

For example, the radiation resistance of a short monopole is from (1-177)

$$R_{r,\text{mono}} = 40\pi^2\left(\frac{h}{\lambda}\right)^2 \qquad \text{for } h \ll \lambda \tag{2-19}$$

where h is the length of the monopole and $\Delta z = 2h$.

The radiation pattern of a monopole above a perfect ground plane, as in Fig. 2-12, is the same as that of a dipole similarly positioned in free space since the fields above the image plane are the same. Therefore, a monopole fed against a perfect ground plane radiates one-half the total power of a similar dipole in free space because the power is distributed in the same fashion but only over half as much

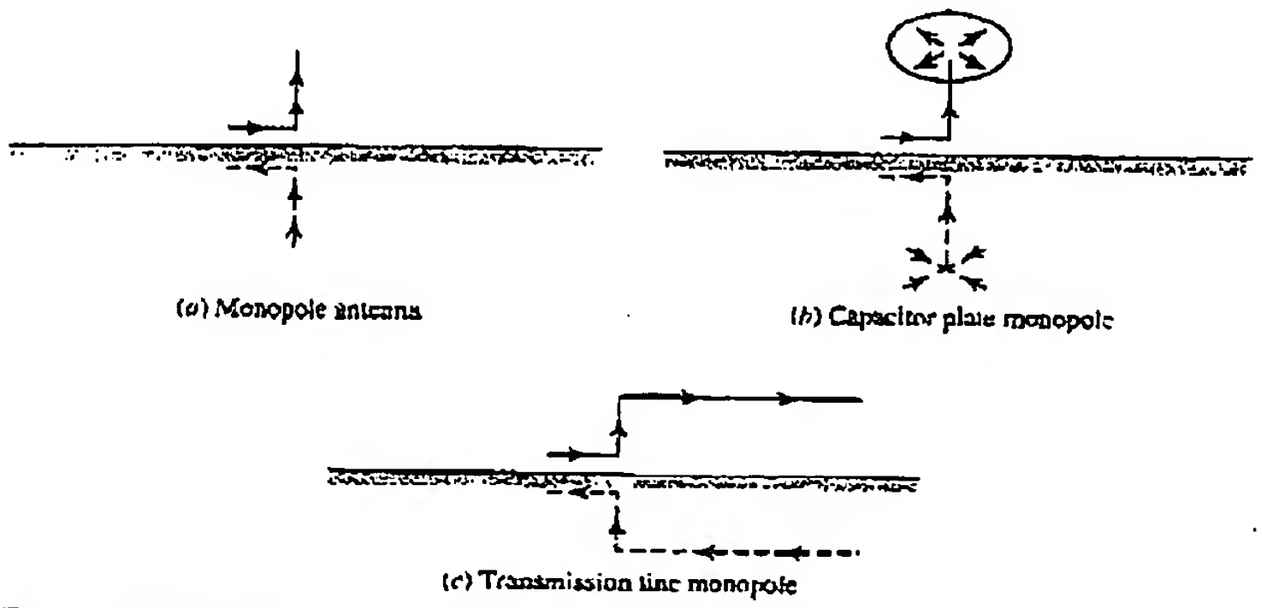

(*a*) Monopole antenna (*b*) Capacitor plate monopole

(*c*) Transmission line monopole

Figure 2-11 Monopole antennas over perfect ground planes with their images (dashed).

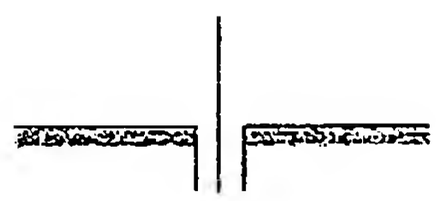

(a) Monopole fed against a large solid ground plane.

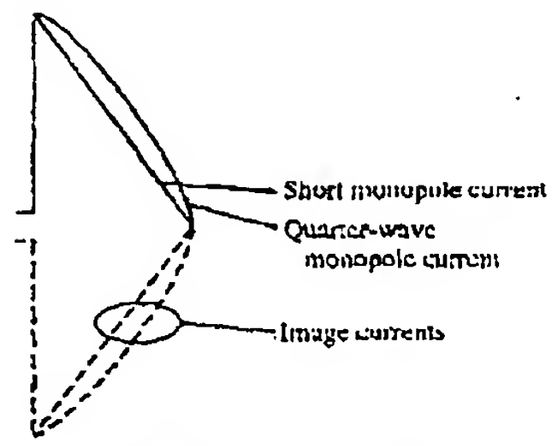

(b) Equivalent dipole model shown with currents.

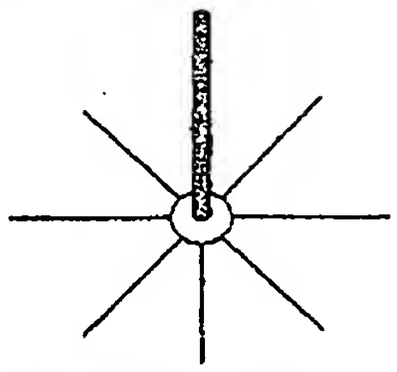

(c) Practical monopole antenna with radial wires to simulate a ground plane.

Figure 2-12 Monopole antennas fed against a ground plane with a coaxial cable.

space. As a result, the beam solid angle of a monopole above a perfect ground plane is one-half that of a similar dipole in free space, leading to a doubling of the directivity:

$$D_{\text{mono}} = \frac{4\pi}{\Omega_{A\,\text{mono}}} = \frac{4\pi}{\frac{1}{2}\Omega_{A\,\text{dipole}}} = 2D_{\text{dipole}} \tag{2-20}$$

This can be shown in another way. If a dipole in free space has a maximum radiation intensity of U_m, a monopole of half the length above a perfect ground plane with the same current will have same value of U_m since the fields are the same. The total radiated power for the dipole is P, so the power radiated from the monopole is $\frac{1}{2}P$. The directivity from (1-145) for the two antennas is

$$D_{\text{dipole}} = \frac{U_m}{U_{\text{iso}}} = \frac{U_m}{P/4\pi} \tag{2-21}$$

and

$$D_{\text{mono}} = \frac{U_m}{\frac{1}{2}P/4\pi} = 2D_{\text{dipole}} \tag{2-22}$$

The directivity increase does not come from an increase in the radiation intensity (and, hence, field intensity) but rather from a decrease in average radiation intensity. This, in turn, comes about because only half the power radiated by a dipole

(a) Monopole with insulators to reduce currents in guys (b) Umbrella-loaded monopole

Figure 2-13 Monopoles with supporting guy wires.

is radiated by a monopole. The directivity of a short monopole, for example, is $2(1.5) = 3$.

The directivity of a quarter-wave monopole is twice that of a half-wave dipole in free space: that is, from Fig. 2-6 and (2-22)

$$D = 2(1.64) = 3.28 = 5.16 \text{ dB} \qquad \textit{λ/4-monopole} \tag{2-23}$$

The input impedance of an infinitesimally thin quarter-wave monopole from Fig. 2-6 and (2-17) is

$$Z_A = \frac{1}{2}(72 + j42.5) = 36 + j21.3\ \Omega \qquad \textit{λ/4-monopole} \tag{2-24}$$

At low frequencies, a monopole that is a quarter wavelength long or less can be rather large physically. For example, in the standard AM broadcast band at 1 MHz, the wavelength is 300 m, and a quarter-wave monopole is 75 m tall. Such a large structure is usually not self-supporting, and guy wires are employed for support. Currents can exist in these guy wires in a downward direction tending to cancel the effect of the vertical element. Insulators are added to break up these currents, as in Fig. 2-13.

If currents are allowed to continue from the monopole out onto the guys, there is a partial top-loading effect for towers shorter than a quarter wavelength, thereby increasing the radiation resistance. See Fig. 2-13*b*. The loading is usually not enough to give uniform current on the vertical member. Also, the downward angle of the guys gives a slight canceling of the fields from the vertical current. For a comparable-length monopole, the umbrella-loaded version has a lower radiation resistance than the capacitor-plate monopole. Experimental data are available in the literature for umbrella-loaded monopoles [3].

2.4 SMALL LOOP ANTENNAS

A closed loop current whose maximum dimension is less than about a tenth of a wavelength is called a **small loop antenna**. Again, small is interpreted as meaning electrically small, or small compared to a wavelength. In this section, we use two methods to solve for the radiation properties of small loop antennas. First, we show that the small loop is the dual of an ideal dipole, and by observing the duality contained in Maxwell's equations, we use the results previously derived for the ideal dipole to write the fields of a small loop. Next, we derive the fields of a small loop directly and show that the results are the same as those obtained using duality.

2.4.1 Duality

Frequently, an antenna problem arises for which the structure is the dual of an antenna whose solution is known. If antenna structures are duals, it is possible to

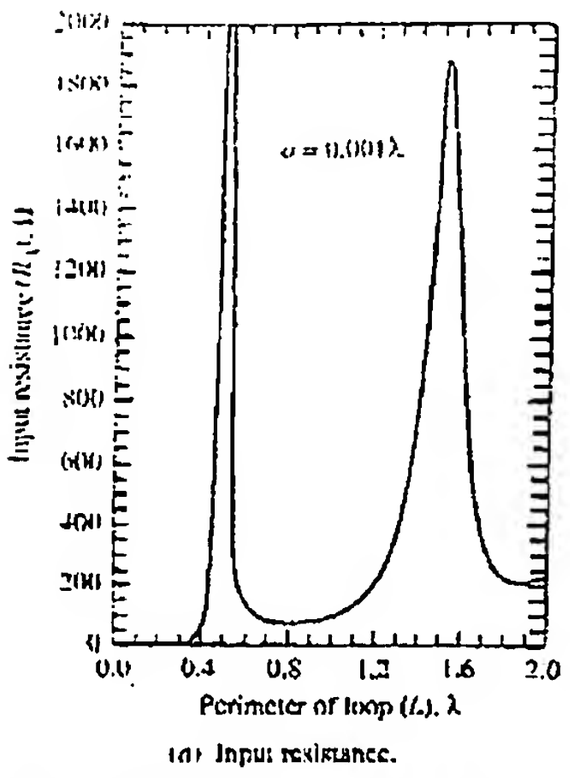

(a) Input resistance.

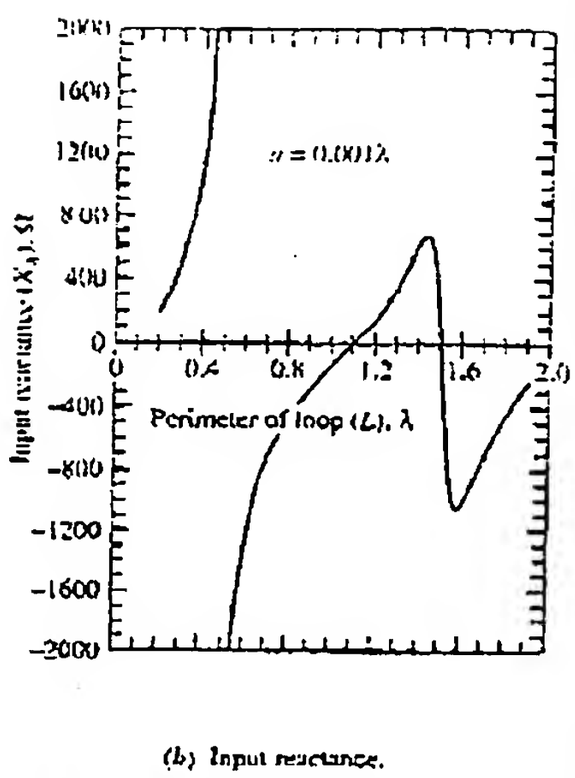

(b) Input reactance.

Figure 5-53 Input impedance of a square loop antenna as a function of the loop perimeter in wavelengths. The loop is fed in the center of one side and has a wire radius of $a = 0.001\lambda$. Numerical calculation methods were used.

5.8 MICROSTRIP ANTENNAS

Printed antennas are constructed using printed circuit fabrication techniques such that a portion of the metallization layer is responsible for radiation. **Microstrip antenna** patch elements, and arrays of patches, are the most common form of printed antenna and were conceived in the 1950s. Extensive investigations of patch antennas began in the 1970s [33, 34] and resulted in many useful design configurations [35]. Printed antennas are popular with antenna engineers for their low profile, for the ease with which they can be configured to specialized geometries, and because of their low cost when produced in large quantities. This section explains the basic operating principles of microstrip elements and arrays. Simple formulas are given that produce approximate results. Lengthy formulas that are more general and more accurate are available [36, 37].

5.8.1 Microstrip Patch Antennas

A microstrip device in its simplest form is a layered structure with two parallel conductors separated by a thin dielectric substrate and the lower conductor acting as a ground plane. If the upper metallization is a long narrow strip, a microstrip transmission line is formed. If the upper conductor is a *patch* that is an appreciable fraction of a wavelength in extent, the device becomes a microstrip antenna, as illustrated in Fig. 5-54. The patch antenna belongs to the class of resonant antennas and its resonant behavior is responsible for the main challenge in microstrip antenna design—achieving adequate bandwidth. Conventional patch designs yield bandwidths as low as a few percent. The resonant nature of microstrip antennas also means that at frequencies below UHF they become excessively large. They are

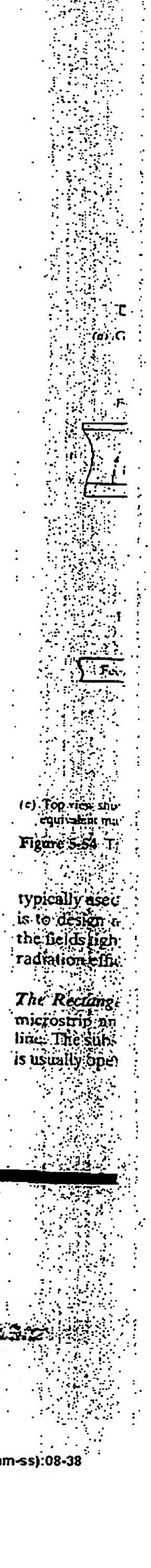

(c) Top view sho
equivalent ma

Figure 5-54 T

typically used
is to design a
the fields high
radiation effic

The Rectang
microstrip an
line. The sub
is usually ope

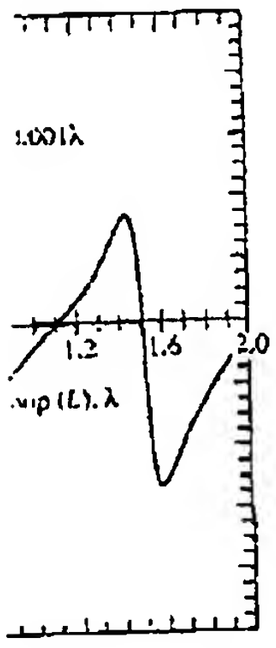

...ductance.

...n of the loop perimeter ...wire radius of $a =$

...cation techniques such ...r radiation. Microstrip ...most common form of ...investigations of patch ...useful design configura... ...ers for their low profile. ...ed geometries, and be... ...his section explains the ...ys. Simple formulas are ..., that are more general

...icture with two parallel ...lower conductor acting ...rrow strip, a microstrip ...h that is an appreciable ...microstrip antenna, as ...ass of resonant antennas ...ge in microstrip antenna ...tch designs yield band... microstrip antennas also ...cessively large. They are

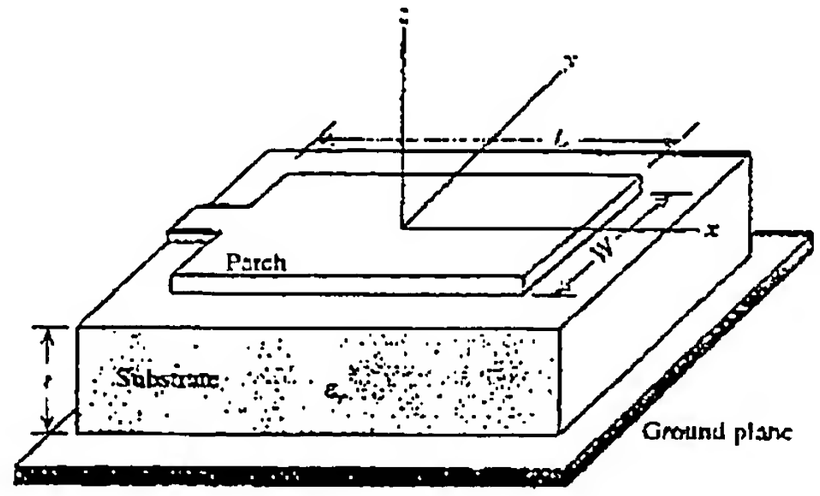

(a) Geometry for analyzing the edge-fed microstrip patch antenna.

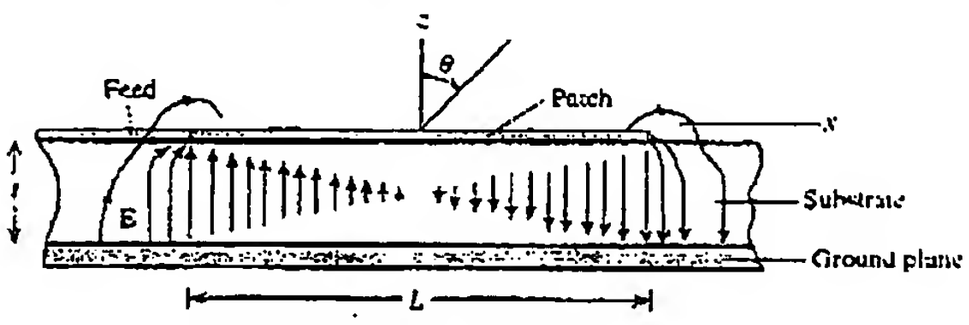

(b) Side view showing the electric fields.

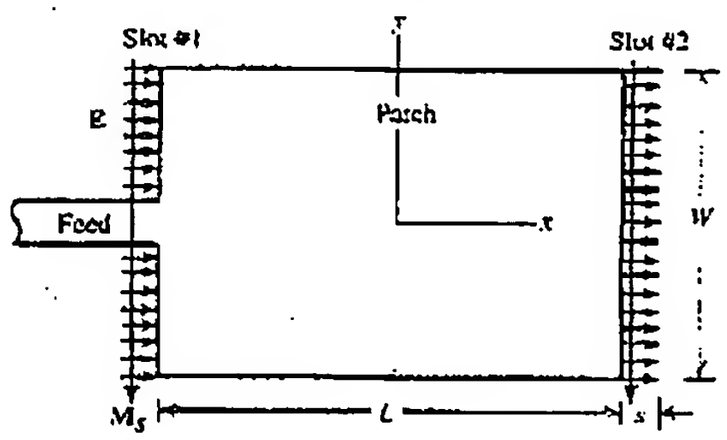

(c) Top view showing the fringing electric fields that are responsible for radiation. The equivalent magnetic surface M_s currents are also shown.

Figure 5-54 The half-wavelength rectangular patch microstrip antenna: $L \approx 0.49\lambda_d$.

typically used at frequencies from 1 to 100 GHz. The tradeoff in microstrip antennas is to design a patch with loosely bound fields extending into space while keeping the fields tightly bound to the feeding circuitry. This is to be accomplished with high radiation efficiency and with the desired polarization, impedance, and bandwidth.

The Rectangular Patch Antenna. Figure 5-54 shows the most commonly used microstrip antenna, a *rectangular patch* being fed from a microstrip transmission line. The substrate thickness t is much less than a wavelength. The rectangular patch is usually operated near resonance in order to obtain a real-valued input impedance.

Models are available for determining the resonant frequency, with the cavity model usually yielding accurate results: see [33]. The fringing fields act to extend the effective length of the patch. Thus, the length of a *half-wave* patch is slightly less than a half wavelength in the dielectric substrate material. This is similar to foreshortening a half-wave dipole to achieve resonance. The amount of length reduction depends on ε_r, t, and W. Formulas are available to estimate the resonant length [33, 36, 37], but empirical adjustments are often necessary in practice. An approximate value for the length of a resonant half-wavelength patch is [34]

$$L \approx 0.49\lambda_d = 0.49\frac{\lambda}{\sqrt{\varepsilon_r}} \qquad \textit{half-wave patch} \tag{5-72}$$

where λ is the free-space wavelength, λ_d the wavelength in the dielectric, and ε_r the substrate dielectric constant. We focus our attention here on the half-wave patch antenna.

The region between the conductors acts as a half-wavelength transmission-line cavity that is open-circuited at its ends. Figure 5-54*b* shows the electric fields associated with the standing wave mode in the dielectric. The electric field lines are perpendicular to the conductors as required by boundary conditions and look much like those in a parallel plate capacitor. The fringing fields at the ends are exposed to the upper half-space ($z > 0$) and are responsible for the radiation. The standing wave mode with a half-wavelength separation between ends leads to electric fields that are of opposite phase on the left and right halves (i.e., positive and negative x). Therefore, the total fringing fields at the edges are 180° out of phase and equal in magnitude. Viewed from the top (see Fig. 5-54*c*), the *x*-components of the fringing fields are actually in-phase, leading to a broadside radiation pattern; that is, the peak radiation is in the $+z$-direction. This model suggests an "aperture field" analysis approach where the patch has two radiating slot apertures with electric fields in the plane of the patch. For the half-wave patch case, the slots are equal in magnitude and phase. The fields along the edges associated with slots 1 and 2 are constant, whereas those along the other edges, seen in side view in Fig. 5-54*b*, have odd symmetry and their radiation cancels in the broadside direction and is usually neglected. The width of the slots is often taken to be equal to the substrate thickness, that is, $s \approx t$. The patch radiation is linearly polarized in the xz-plane, that is, parallel to the electric fields in the slots.

The pattern of a rectangular patch antenna is rather broad with a maximum direction normal to the plane of the antenna. Pattern computation for the rectangular patch is easily performed by first creating equivalent magnetic surface currents, as shown in Fig. 5-54*c*, from the fringe electric fields using $\mathbf{M}_s = 2\mathbf{E}_a \times \hat{\mathbf{n}}$, where $\mathbf{E}_a$ is the fringe electric field in each of the edge slots; this follows from (1-23) or (7-2). The factor of 2 comes from the image of the magnetic current in the electric ground plane (see Fig. 7-4*c*) if we assume t is small. The far-field components follow from (7-26) (see Prob. 7.1-7) as

$$E_\theta = E_a \cos\phi\, f(\theta, \phi) \tag{5-73a}$$

$$E_\phi = -E_a \cos\theta \sin\phi\, f(\theta, \phi) \tag{5-73b}$$

where

$$f(\theta, \phi) = \frac{\sin\left[\frac{\beta W}{2}\sin\theta\sin\phi\right]}{\frac{\beta W}{2}\sin\theta\sin\phi}\cos\left(\frac{\beta L}{2}\sin\theta\cos\phi\right) \tag{5-73c}$$

and β is the usual free-space phase constant. The first factor is the pattern factor for a uniform line source of width W in the y-direction. The second factor is the array factor for a two-element array along the x-axis corresponding to the edge slots; see (3-8). The patch length L for resonance is given by (5-72). The patch width W is selected to give the proper radiation resistance at the input, often 50 Ω. The principal plane patterns follow from (5-73) as

$$F_E(\theta) = \cos\left(\frac{\beta L}{2}\sin\theta\right) \qquad E\text{-plane, } \phi = 0° \qquad (5\text{-}74a)$$

$$F_H(\theta) = \cos\theta\,\frac{\sin\left[\frac{\beta W}{2}\sin\theta\right]}{\frac{\beta W}{2}\sin\theta} \qquad H\text{-plane, } \phi = 90° \qquad (5\text{-}74b)$$

This simple pattern expression neglects substrate effects and slot width (i.e., fringing).

Typical input impedances at the edge of a resonant rectangular patch range from 100 to 400 Ω. An approximate expression for the input impedance (reactance is zero at resonance) of a resonant edge-fed patch is [36]

$$Z_A = 90\,\frac{\varepsilon_r^2}{\varepsilon_r - 1}\left(\frac{L}{W}\right)^2\ \Omega \qquad \textit{half-wave patch} \qquad (5\text{-}75)$$

Thus, the input impedance (resistance) is reduced by widening the patch. For example, for a dielectric of $\varepsilon_r = 2.2$, a width-to-length ratio of $W/L = 2.7$ gives a 50-Ω input impedance.

Techniques for feeding patches are summarized in Fig. 5-55. They can be classified into three groups: directly coupled, electromagnetically coupled, or aperture coupled. Direct coupling methods are the oldest and most popular, but only provide one degree of freedom to adjust impedance. The microstrip feed line exciting the patch edge and the coaxial probe are examples of direct feeds. The rectangular patch is normally fed along a patch centerline in the E-plane as shown in Fig. 5-55. This avoids excitation of a second resonant mode orthogonal to the desired mode, which would lead to excessive cross polarization.

The direct coaxial probe feed illustrated in Fig. 5-55*a* is simple to implement by extending the center conductor of the connector attached to the ground plane up to the patch. Impedance can be adjusted by proper placement of the probe feed. As the probe distance from the patch edge, Δx_p in Fig. 5-55*a*, is increased, the input resistance of (5-75) is reduced by the factor $\cos^2\frac{\pi\,\Delta x_p}{L}$ [36]. A disadvantage of the probe feed is that it introduces an inductance that prevents the patch from being resonant if t is 0.1λ or greater. Also, probe radiation can be a source of cross polarization.

The microstrip feed of Fig. 5-54 is planar, permitting the patch and feed to be printed on a single metallization layer. This feed approach is especially well suited to arrays where the feed network can be printed with the elements. Changing the patch width, as determined with (5-75), to control impedance is often not convenient. However, the impedance of the edge-fed patch can be transformed by using a quarter-wave matching section of microstrip transmission line as shown in Fig. 5-55*b*. That is, the antenna input impedance Z_A can be matched to a transmission line of characteristic impedance Z_c (often 50 Ω) with a section of transmission line

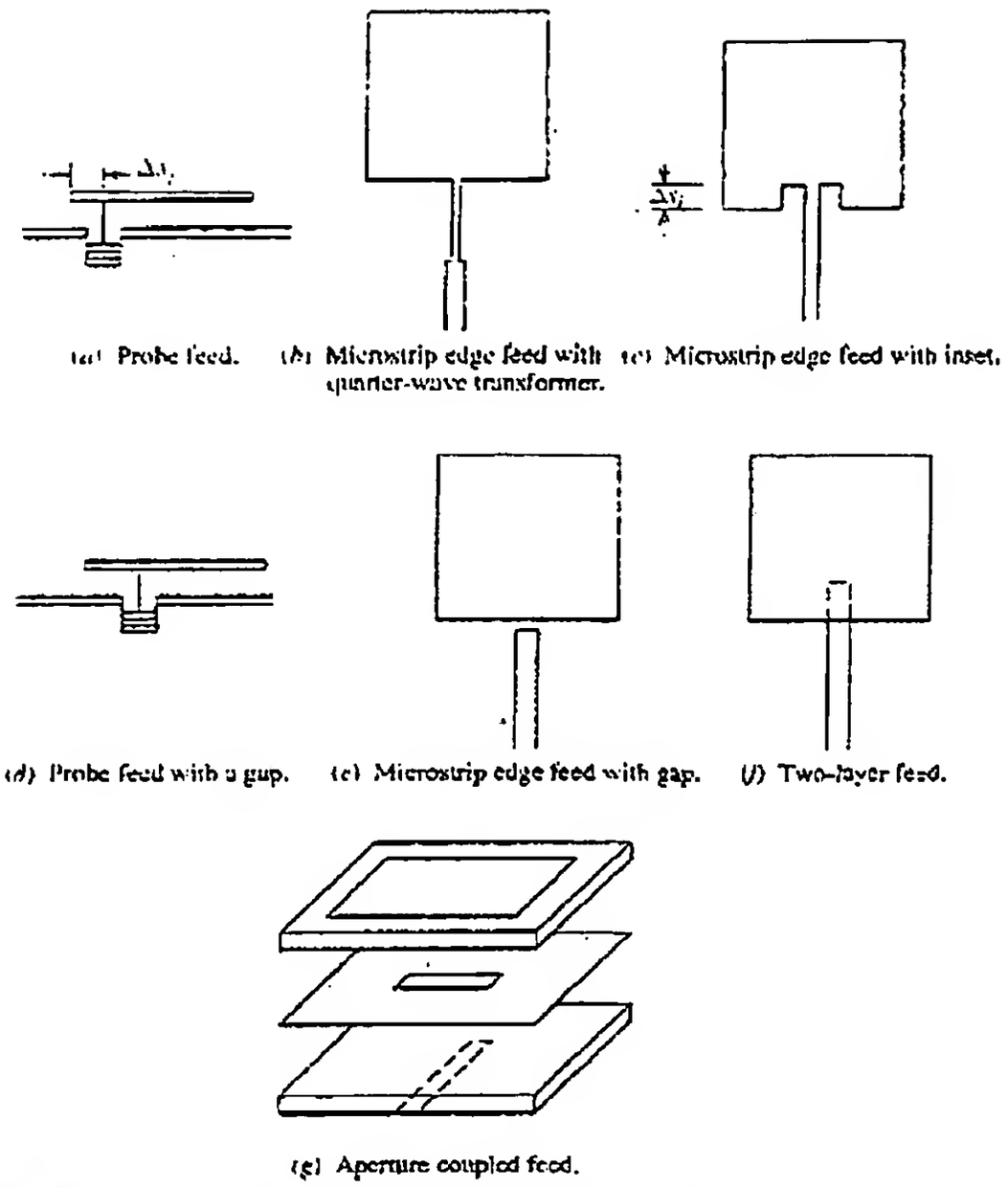

(a) Probe feed. (b) Microstrip edge feed with quarter-wave transformer. (c) Microstrip edge feed with inset.

(d) Probe feed with a gap. (e) Microstrip edge feed with gap. (f) Two-layer feed.

(g) Aperture coupled feed.

Figure 5-55 Techniques for feeding microstrip patch antennas.

that is a quarter-wavelength long based on the wavelength in the transmission line. This characteristic impedance of the matching section is given by

$$Z'_{in} = \sqrt{Z_A Z_{in}} \qquad \textit{quarter-wave transformer} \tag{5-76}$$

In general, the characteristic impedance of a microstrip line is decreased by increasing the strip width, much as loss resistance is inversely proportional to wire diameter: see (1-175). That is, the wider the strip, the lower the characteristic impedance.

Another type of microstrip feed is the inset feed shown in Fig. 5-55*c*, which offers the advantage of being planar and easily etched as well as providing adjustable input impedance through inset geometry changes. The input resistance of (5-75) is multiplied by the factor of $\cos^2 \frac{\pi \Delta x_i}{L}$ [33]. However, large input impedance changes that are required for high-permittivity substrates demand significant inset depths, which affects cross polarization and radiation pattern shape.

The direct feeds of Figs. 5-55*a* through 5-55*c* have a narrow bandwidth that can

only be increased by increasing the p... waves. Electromagnetically coupled feeds do not co... have the advantage of being planar and easily etched as well as providing adjustable input impedance through inset geometry changes. The input resistance of (5-75) is multiplied by the factor of $\cos^2 \frac{\pi \Delta x_i}{L}$ [33]. However, large input impedance changes that are required for high-permittivity substrates demand significant inset depths, which affects cross polarization and radiation pattern shape.

The direct feeds of Figs. 5-55*a* through 5-55*c* have a narrow bandwidth that can only be increased by increasing the p... waves. Electromagnetically coupled feeds (Figs. 5-55*d* through 5-55*f*. The probe... Also, the gap-cou... substrates. The m... etch. However, ... The two-layer fe... microstrip-to-mi... strip feed offers...

The aperture-... substrate can be... strate containing... the fields to the... is that the optra...

Materials such... substrate with ε... [33: 38, Chap. 5]... and dimensional... and available sh...

The bandwidt... thickness t and l... increase in the... array of patches... ultimate limiting... ple empirical for...

where bandwidt... for a VSWR les... square patch for... bandwidth from... in (5-77).

Another rect... element that has... the ground plan... $x > 0$. The corre... wave patch.

EXAMPLE 5-2 Half-W...

A square half-w... cm (45 mils) thick...

with inset.

:r feed.

in the transmission line.
ven by

rimer (5-76)

- is decreased by increas-
irtional to wire diameter.
acteristic impedance.
n Fig. 5-55c, which offers
roviding adjustable input
distance of (5-75) is mul-

nput impedance changes

; significant inset depths.
ce.
.rrow bandwidth that can

only be increased by increasing the substrate thickness, which has the drawback of increasing the power in the waves trapped along the surface, which are called *surface waves*. Electromagnetic coupled feeds (also called proximity, noncontacting, or gap feeds) do not contact the patch and have at least two design parameters. They also have the advantage of being less sensitive to etching errors. For each direct feed in Figs. 5-55*a* through 5-55*c*, there is gap feed counterpart shown in Figs. 5-55*d* through 5-55*f*. The probe feed with a gap in Fig. 5-55*d* has the advantages of coaxial feeds. Also, the gap capacitance partially cancels the probe inductance, permitting thicker substates. The microstrip feed with a gap in Fig. 5-55*e* is entirely planar and easy to etch. However, in high-permittivity designs, the gap distance may become small. The two-layer feed of Fig. 5-55*f* is a recent technique that is especially useful in microstrip arrays with a top layer for the patches and a second layer for the microstrip feed network.

The aperture-coupled feed of Fig. 5-55*g* is increasing in popularity. The upper substrate can be of low dielectric constant to promote radiation and a lower substrate containing the feed can be of high dielectric constant to enhance binding of the fields to the feed lines. This leads to increased bandwidth. Another advantage is that the central ground plane acts to isolate the feed system from the patches.

Materials such as PTFE composites and alumina are available for the dielectric substrate with ε_r ranging from 1 to about 25, with around 2.5 being most popular [33; 38, Chap. 3]. The selection of dielectric type is based on its loss, temperature and dimensional stability, uniformity of manufacturing (especially ε_r variations), and available sheet sizes and thicknesses.

The bandwidth and efficiency of a patch are increased by increasing substrate thickness t and by lowering ε_r. The associated penalty in array applications is an increase in side lobes and cross polarization as a result of surface waves across an array of patches. This is a fundamental design tradeoff. Bandwidth is often the ultimate limiting performance parameter and can be found from the following simple empirical formula for impedance bandwidth [36]:

$$B = 3.77 \frac{\varepsilon_r - 1}{\varepsilon_r^2} \frac{W}{L} \frac{t}{\lambda} \qquad \frac{t}{\lambda} \ll 1 \tag{5-77}$$

where bandwidth is defined as fractional bandwidth relative to the center frequency for a VSWR less than 2:1. For example, at an operating frequency of 3.78 GHz, a square patch on a substrate of $\varepsilon_r = 2.2$ with $t = 1/16$ in. (1.59 mm) = 0.02λ, the bandwidth from (5-77) is 1.9%. The bandwidth dependence on thickness t is evident in (5-77).

Another rectangular patch antenna encountered in practice is the quarter-wave element that has $L \approx \lambda_d/4$ and is formed by placing shorting bins from the patch to the ground plane at $x = 0$ in Fig. 5-54*a* and eliminating the patch metalization for $x > 0$. The current peak (electric field null) is then in the same position as the half-wave patch.

EXAMPLE 5-2 *Half-Wave, Square Microstrip Patch Antenna*

A square, half-wave patch was designed to resonant at 3.03 GHz ($\lambda = 9.9$ cm) on a $t = 0.1143$ cm (45 mils) thick substrate with $\varepsilon_r = 2.35$. From (5-72),

$$L = W = 0.49 \frac{\lambda}{\sqrt{\varepsilon_r}} \approx 0.49 \frac{9.9}{\sqrt{2.35}} = 3.16 \text{ cm} \tag{5-78}$$

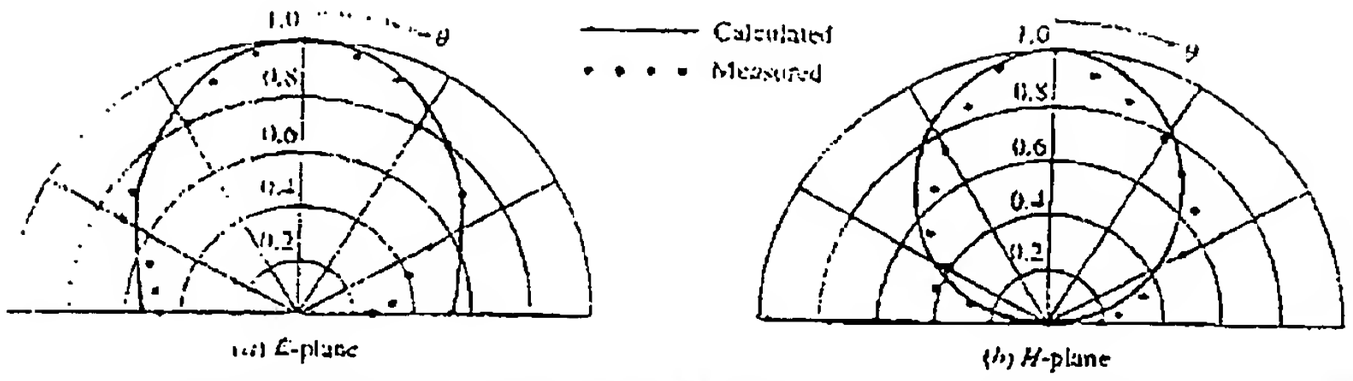

Figure 5-56 Radiation patterns for the square microstrip patch of Example 5-2 calculated (curves) using (5-74) and measured (points).

From (5-75), the input impedance is $Z_A = 368\ \Omega$, which compares to a measured value of 316 Ω at resonance. The measured resonant frequency of 3.01 GHz compares very well with the design frequency of 3.03 GHz. The radiation patterns in the principal planes are given by (5-74). These patterns are plotted in Fig. 5-56 together with data measured at Virginia Tech. The agreement is very good for the simple theory employed.

Other Patch Shapes. There are many patch shapes for special purposes [35]. Important among these are patches for creating circular polarization. Circular polarization can be achieved by feeding the corner of a square patch, by feeding adjacent orthogonal edges of a square patch 90° out-of-phase, or by using a pentagonal shaped patch. A number of software packages are available for analyzing the currents, impedance, and radiation from microstrip elements of most any shape as well as small arrays of patches with the feed network.

5.8.2 Microstrip Arrays

Arrays of microstrip antennas offer the advantage that the feed network as well as the radiating elements can be printed, often by fabrication on the same single layer printed circuit board. More sophisticated implementations are finding wide use in many system applications that fully integrate microstrip radiating elements and feed lines along with the transmitting and receiving circuitry. In fact, antenna technology is following an evolutionary path similar to that of electronics, moving from discrete devices that are individually connected to an antenna element toward full integration where chips are integrated with the feed lines and radiators.

Microstrip antennas are often used in one of many possible array configurations. Microstrip arrays are very popular for fixed-beam applications because the radiating elements and feed network can be fabricated on a single-layer printed circuit board using low-cost lithographic techniques. Interelement spacings for fixed-beam applications are usually chosen to be less than free-space wavelength (λ) to avoid grating lobes and greater than $\lambda/2$ to provide sufficient room for the feed lines, to achieve higher gain for a given number of elements, and to reduce mutual coupling. The active element patterns shown in Fig. 3-30 are very similar, indicating that mutual coupling effects are not significant for those microstrip patches that are spaced 0.5λ apart.

Largely as the result of pioneering work for sophisticated military radar, phase-scanned microstrip arrays can be produced with monolithic microwave integrated circuit (MMIC) techniques that fabricate amplifiers, phase shifters, and other de-

vices on the s
planar, or cont
fed, planar mic
We illustrate
4" elements w
uniform amplit
illustrates imp
work. Figure 5
build up very l
that are of equ
citation phase
has $\epsilon_r = 2.2$ s
directions is d
$L = 0.49\lambda_d = 0.$
to solve for the

Impedance m
pedance microst
uses two divide
50-Ω input impe
$Z_A = 200\ \Omega$ as ma
impedances of 2(
matched to the
Combining this i
be connected fro
in Fig. 5-57*b*, and
rays to build up
$\sqrt{50 \cdot 100} = 70$
bandwidth limita
Arrays similar
for $N = 16, 64, 25$
$d = 0.8\lambda$ is easily

$$G = \varepsilon_{ap} \frac{4\pi}{\lambda^2} A_p =$$

$$\approx \varepsilon_{ap} \frac{4\pi}{\lambda^2} N(0.$$

Since the array is
100%. However, u
face waves, and dis
gain was close to t
elements [39]. This
reflector of the sam
experience significa
less than 50%.